Stanisław CHUDZIK

ORCID: 0000-0002-8433-0274

DOI: 10.15199/48.2025.05.03

Detection of defects in natural leather using active thermography

Wykrywanie wad skóry naturalnej metodą termografii aktywnej

***Abstract**. This article presents a method for detecting defects in the internal and surface structure of tanned natural leather, especially grain leather. Presented method is based on application of a linear infrared radiator to obtain an impulse-like (in time) thermal input and measuring output temperature transients on tested surface using an infrared camera. The paper presents selected results obtained from experiments. The presented solution is a part of a project aimed at developing an industrial device for non-destructive evaluation and detection of defects in natural leather.*

***Streszczenie.** W artykule przedstawiono metodę wykrywania defektów w strukturze wewnętrznej i powierzchniowej garbowanej skóry naturalnej, zwłaszcza skóry licowej. Przedstawiona metoda opiera się na zastosowaniu liniowego promiennika podczerwieni do uzyskania impulsowego (w czasie) wymuszenia cieplnego i pomiarze zmian temperatur na badanej powierzchni za pomocą kamery termowizyjnej. W artykule przedstawiono wybrane wyniki uzyskane z eksperymentów. Przedstawione rozwiązanie jest częścią projektu mającego na celu opracowanie przemysłowego urządzenia do nieniszczącej oceny i wykrywania defektów w skórze naturalnej.*

Keywords: thermal diffusion, natural leather, active thermography
Słowa kluczowe: dyfuzja cieplna, skóra naturalna, aktywna termografia

Introduction

Over the years, the industry of exclusive products made of natural leather has been exhibiting continuous growth. Customers still appreciate advantages of genuine leather such as durability, flexibility and good breathability.

Unlike for example plastics, natural leather has inhomogeneous structure and various properties depending on an animal species and method of tanning. Manufacturers of upholstered furniture use finished leather obtained by tanning animal raw hide and skin primarily from cattle, but also from pigs, goats, sheep and horses. Tanning is a process of treating in which chemical agents or natural extracts are applied to raw hides and skins in order to prevent rotting and impart the tanned leather desirable features such as softness, flexibility, durability, waterproofing etc. Quality and properties of leather depend mainly on an animal from which the leather was obtained.

The most common way of leather inspection currently used is subjective manual and visual evaluation: a sheet of tanned leather is laid out on a table or a stand and a worker looks for flaws of the leather surface and structure using his/her sight and touch. The leather can also be stretched in all directions in order that flaws of the internal structure became better visible on the surface.

Some attempts are being made to make the inspection process faster and automatic, for example a sheet of leather is unfolded on a table and a digital camera takes photos of the leather surface in visible light. Then digital image processing of the photos is applied to detect and mark areas of flaws visible on the surface, where the leather might not satisfy quality requirements.

The most commonly used non-destructive inspection technique [1] that uses infrared radiation to detect material defects is active infrared thermography [2, 3, 4]. Active thermography testing is usually carried out in two stages: experimental and data analysis. On the experimental stage, a material under test, usually a specially prepared sample, is heated using sources of particular thermal input, typically radiators of controlled power [5]. The thermal output of the heated surface is recorded by an infrared camera [6] during and after the input as a time sequence of thermograms. This sequence of thermograms is a record of transient temperature field of the sample surface limited to the experiment time window. Transient temperature field is a material thermal response in heat exchange conditions specified in the experiment. To record a thermogram sequence the infrared camera must be equipped with a frame-grabber unit and software managing thermogram acquisition process [5, 7, 8]. The software usually has options to specify recording parameters such as sampling frequency, object parameters (e.g. band emissivity) and measurement conditions (e.g. atmosphere temperature) [9].

On the data analysis stage the recorded sequence of thermograms is digitally processed to reveal potential under-surface anomalies. Conventional methods of digital image and signal processing are used, such as filtering, edge detection, segmentation etc. [2, 5,10], as well as more advanced methods, such as classification, regression etc. [7, 8, 11], based on machine learning and artificial intelligence [12]. The conventional image processing algorithms are applied to the thermogram sequence analysis first of all to increase thermal contrast in the camera field of view in order either to make it easier for a human quality controller to notice defects or to improve efficiency of further automatic recognition algorithms. When using advanced methods, the conventional methods are usually used as initial image pre-processing. Finally, the data analysis provides diagnostic information about if and where there are defects in the tested material.

Recently, active thermography has been applied to evaluation of more complex materials such as composites [7, 8]. Leather, like composites, is also an inhomogeneous material. In particular, its thermal properties are anisotropic due to complex fibrous structure, variable content of water etc. In materials of this type, detection of the defects mentioned above is much more difficult.

This article presents a method for detecting defects in a leather sample. It is based on processing data obtained by measuring transients of temperature field on leather surface. The algorithm works in the time domain and uses the whole temperature transients recorded for the same pixels (single surface points) of the whole thermogram sequence.

Laboratory setup with linear infrared radiator

A sheet of leather to be inspected is laid out and made as smooth as possible on a flat table and then the leather is heated by a linear infrared radiator mounted on a moving frame above the table and shifted along the table. During one run the radiator produces a short impulse-like (in time) thermal input to successive passed strips of the upper leather surface. Temperature changes of the upper surface (thermal response) during the thermal input and afterwards, for some time of free self-cooling, are measured touch less by a digital infrared camera and recorded in a computer as a sequence of thermograms. A thermogram is a matrix of temperature values at all points at the same time instant.

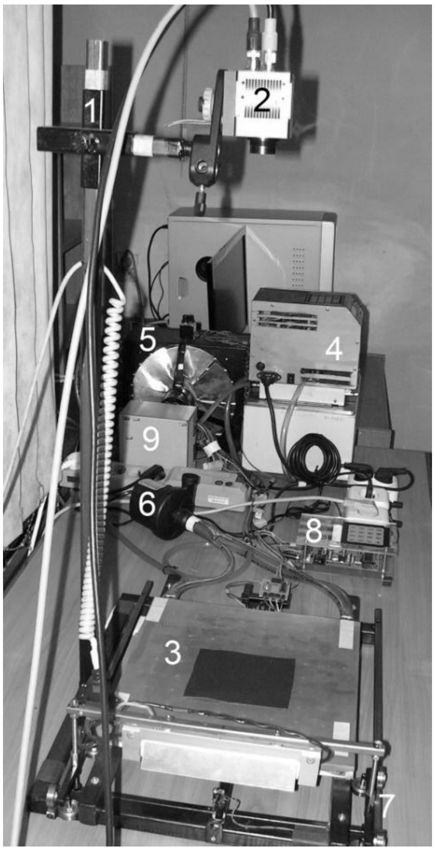

Fig. 1. Laboratory setup

A photo of the laboratory setup is shown in figure 1. The IRS336-NDT infrared camera 2 is mounted on stand 1. The camera can record up to 60 thermograms per second using the manufacturer software. Below there is a special aluminium table for laying out a sheet of leather to be inspected. The camera field of view (FOV) covers almost the whole leather sample. The table panel can be fluid cooled. The fluid circulation system includes a pump, thermostat 4 and cooler 5 with a fan. To ensure uniform and tight fitting of the leather, the air from between the table and the lower surface of the leather is sucked off through small holes in the table top by air pump 6. Angular speeds of the cooler fan and the air pump can be smoothly adjusted. A movable frame over the table is a part of carriage 7 that can move along the table. An infrared lamp or other heat source can be attached to the carriage frame and produce a thermal input to the leather on the table. The power of the heat source can also be adjusted smoothly. The carriage is driven by a stepper motor and a cogged belt and equipped with two mechanical limit switches and two optical sensors for triggering recording of thermograms at a specified position of the carriage (positions of the optical sensors along the carriage rail can be changed). Functioning of the setup, i.e. controlling the carriage drive, generating triggering signals for thermogram recording, switching the heat source and the air pump, is controlled by microprocessor system 8, based on AT89S253 microcontroller. The carriage motor and the cooler fan are supplied from 12V power supply 9. An additional frame with unwoven fabric of high thermal emissivity can be mounted at the top of the stand to limit the influence of environmental conditions. If necessary, a normal camera operating in visible light can be added to the setup to extend the research by making fusion of data from infrared images and standard photos.

Test samples

The experiments were carried out using samples of natural leather delivered by a renowned manufacturer of upholstered furniture. Experts from the manufacturer quality department indicated and classified defects on 12 samples provided for testing. The samples were tanned, smooth, mostly cattle grain leather, with protective layer, surface dyed, satin finished, 1 to 2 mm thick.

Due to great amount of experimental data, only representative results obtained for three selected leather samples shown on photo in figure 2, are discussed in the paper. Sample 1 is smooth, tanned cattle grain leather with protective layer, surface dyed, satin finished, 2 mm thick, with defects defined as stretch marks. Sample 2 is smooth, tanned cattle grain leather with protective layer, surface dyed, satin finished, 2 mm thick, with defects defined as insect (cattle fly) bites marks. Sample 3 is smooth, tanned goat grain leather, surface dyed, shiny finished, 1 mm thick, with defects defined as arisen during tanning.

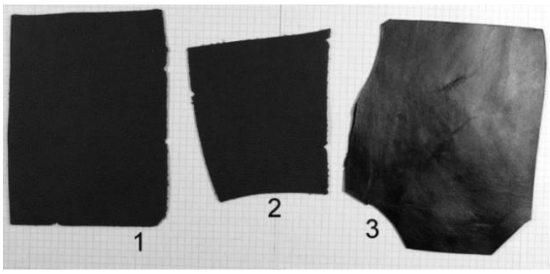

Fig. 2. Samples of natural weather selected for discussion

Equivalent sequences of thermograms

During the movement of the linear heat source, the heat diffusion process recorded for successive columns of thermogram pixels is shifted in time. The impulse-like heating takes place when the carriage (and the heat input) reaches a given position along the table (along X-axis). Direct processing of a thermogram sequence obtained in such conditions is unreasonable because temperature and temperature gradient on the free cooling surface decrease with time. Consequently, instead of detecting differences due to material defects, the algorithm would mainly show on later images differences due to the advance of the cooling process in successive column areas of the sample, depending on x-coordinate.

That is why sequences of thermograms were processed to obtain images equivalent to those that would be recorded using a fixed radiator that lights simultaneously the whole sample surface. To achieve this, we need to determine how much time it takes for the temperature maximum to move from the first (most left) to the last (most right) column of images in the sequence. It provides time t_{xmax} after which the temperature maximum occurs at position x_m (it is assumed that t_{xmax}= 0 at x = 1) and time t_x of the full run of the linear heat source along the table. Next, each of n thermograms $TRG(i)$ creating the sequence, where the time index $1 \leq i \leq n$, is divided into columns of pixels $KP(i,x)$, where the position coordinate $1 \leq x \leq 320$ (the infrared camera resolutionis 320x240). Now, equivalent images $ETRG(j)$, where: $1 \le j \le k$, $j=i - t_{xmax}$, $k = n - t_{xmax}$, are made up of the original columns of pixels, so that the columns of the equivalent images $EKP(j,x_e) = KP(i = j + t_{xmax}, x = x_e+x_m)$.Of course, number k of the created equivalent thermograms for $t_{xmax}> 0$ is less than n. If the carriage speed is such that the travelling time from position x to $x + 1$ is not exactly equal to the camera sampling time $t_s = t(i+1) - t(i)$, some interpolation (e.g. linear) should be applied to calculate instantaneous temperature of pixels ("between" two recorded thermograms) in equivalent column $EKP(j, x)$.

Experimental results

In the example experiment discussed below the camera recorded $n = 600$ thermograms of 320x240 pixels in 20 seconds with sampling frequency $f_s = 30$ images per second. An example thermogram recorded after 2 seconds from the start of scanning (i.e. for $j = 60$) is presented in figure 3. The dashed rectangle is an outline of the infrared radiator, which is travelling leftwards during recording with speed v. The plot of temperature versus time recorded on successive thermograms during the full radiator run is shown in figure 4 for the pixel marked in figure 3.

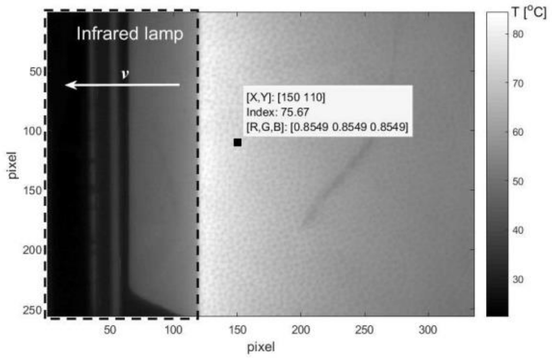

Fig. 3. Thermogram of the tested sample recorded for time $t = 2$ s

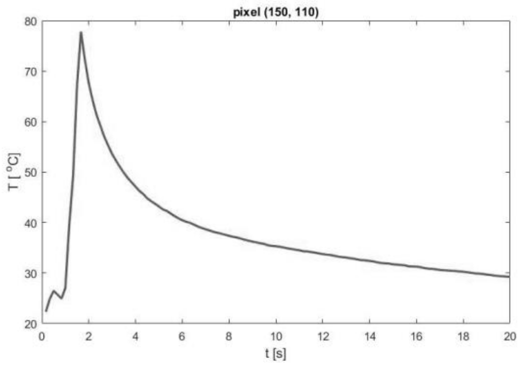

Fig. 4. Plot of temperature versus time recorded in the sequence of thermograms for the pixel marked in figure3. For 0.5s < t < 1.7s (growing slope) the heated strip of the sample is covered by the radiator casing

The temperature versus time plot for each pixel can be divided into three parts: 1) low temperature before the radiator arrival, 2) short time of heating when the radiator is travelling over a pixel, 3) self-cooling phase. The heating stage cannot be analysed because the pixel is then covered by the radiator casing, so only the self-cooling phase data will be taken for further analysis. Note that since the linear heat source is set parallel to Y-axis of the image and moving along X-axis, the thermal input occurs at the same time for pixels of the same x-coordinate (columns of image pixels). For pixels of the same y-coordinate (rows of image pixels) the thermal input time is delayed proportionally to their x-coordinate and inversely proportional to the radiator speed. Figure 5 shows two examples of equivalent thermograms obtained for sample 1.

a)

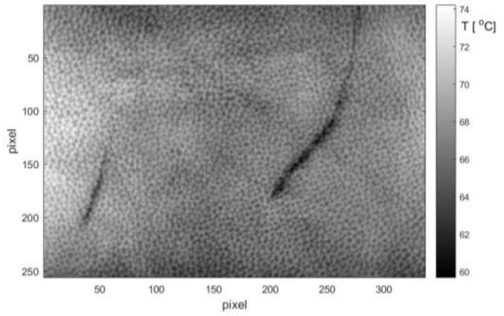

b)

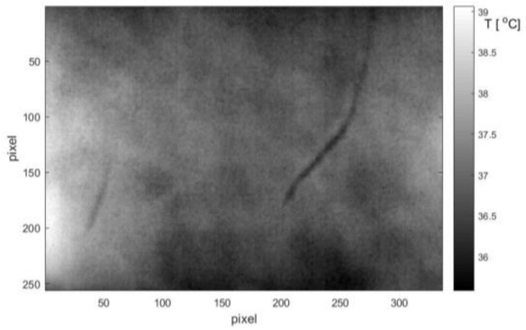

Fig. 5. Examples of equivalent thermograms obtained for sample 1: a) $ETRG(j = 12)$, b) $ETRG(j = 200)$

Processing of leather surface temperature transients

First, temperature waveforms for each pixel $TETRG(x,y,j)$, where $1 \le j \le k$ is the time index, were smoothed and "downsampled" by replacing short sequences of 5 successive temperature samples with their averages:

(1) $$T_{SETRG}(x,y,i) = \frac{\sum_{j=1+(i-1)*5}^{j=i*5} T_{ETRG}(x,y,j)}{5}, \quad 1 \le i \le \left(\frac{k}{5}\right).$$

The averaging is repeated with step 5 which reduces the sequence length to $m=k/5$. The filtering reduces not only computing load but also the noise from the camera array of non-cooled microbolometric detectors [6, 9]. The next step after filtering in the time domain is filtering in the image (spatial) domain. In the presented algorithm the 2D local lowpass (blurring) filter with a square kernel 21x21 pixels (dxy=21), with all pixel values $m_{xy}=1/d_{xy}^2$, was used:

(2) $$T_{TTRG}\,(x,y,i) = \frac{\sum_{p=x-10}^{p=x+10}\sum_{q=y-10}^{q=y+10} T_{SETRG}(p,q,i)}{21^2}, \quad 1 \le p \le 320, 1 \le q \le 240, 1 \le i \le m$$

For pixel index p or q in (9) out of the thermogram image range, the corresponding component was discarded (pixel temperature was assumed zero) and the denominator was decreased by 1. Suitable choice of the kernel size d_{xy} will be considered in further research. Images obtained after the low pass filtering represent no uniformities with low temperature gradient. They will be called background thermograms and denoted as $TTRG(i)$, where $1 \le i \le m$ is the time index. An example background thermogram of sample 1 for $i = 2$ is shown in figure 6.

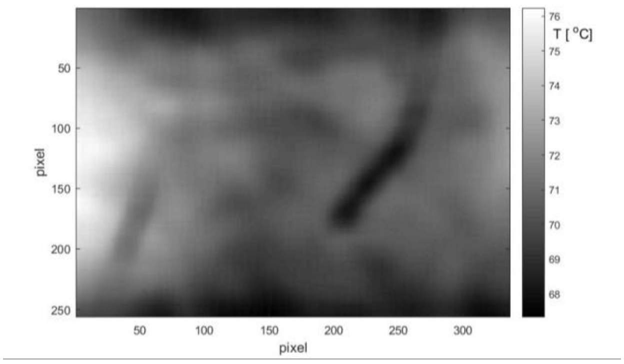

Fig. 6. Example background thermogram $TTRG(i=2)$ of sample 1

The next step is to compute difference images $RTRG(i)$, $1 \leq i \leq m$, defined as the squared difference of a background thermogram and corresponding equivalent thermogram:

$$(3) \qquad RTRG(i) = (TTRG(i) - ETRG(i))^2, \ 1 \leq i \leq m.$$

Difference image $RTRG(i=2)$ of sample 1 is presented in figure 7.

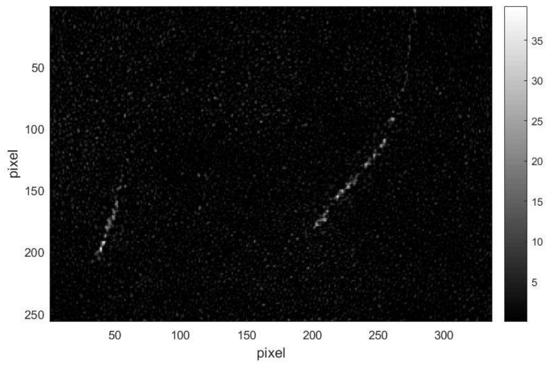

Fig. 7. Difference image $RTRG(i=2)$ of sample 1

In order to take into account temperature equalization due to heat diffusion, the average squared temperature difference is calculated for each difference image:

$$(4) \qquad T_{STRG}(i) = \frac{\sum_x \sum_y T_{RTRG}(x,y,i)}{320*240}, \ \ 1 \leq i \leq m.$$

Assuming that later thermograms do not contribute much information about inhomogeneity of the sample structure (it is only a steady state heat diffusion), the observation horizon was shortened to time $t(i_p)$,for which $TSTRG(i_p) \leq$ TSTRG$(i=1)$/10. The squared temperature differences of difference images (3) are then divided by corresponding (i.e. at the same time) image averages (4). It gives a shortened sequence of relative difference images:

$$(5) \qquad WTRG(i) = RTRG(i)/T_{STRG}(i), \ \ 1 \leq i \leq p.$$

In order to obtain one image showing all potential defects that could become visible at different instants of the heat diffusion process, the algorithm assigns to each pixel (x,y) the maximum relative squared temperature difference calculated for this pixel from sequence (5):

$$(6) \qquad T_{MTRG}(x,y) = \max\left(T_{WTRG}(x,y,i)\right), 1 \leq i \leq p$$

Figure 8 shows an example image T_{MTRG}, composed of time maxima (6), for sample 1.

The final step is image binarization where the key issue is choice of a threshold. It is assumed that when leather defects occur on an image, a number of pixel values close to some relative squared temperature difference T_{MTRG} increases. Such an increase can be detected from an image histogram. Therefore the algorithm calculates an image histogram for n = 100 bins and searches for its first minimum starting from zero. The central value of the bin of the found minimum is taken as the image binarization threshold – it is shown in figure 9. An example binary image, obtained for sample 1, is shown in figure 10.

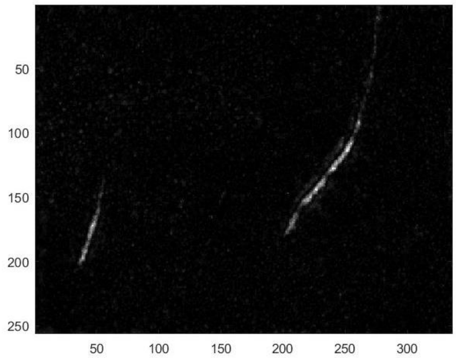

Fig. 8. Example maxima image T_{MTRG} obtained for sample 1

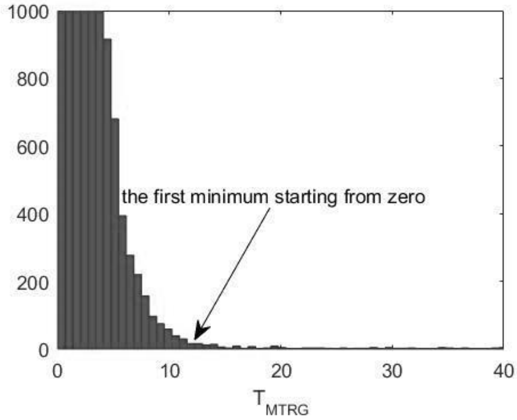

Fig. 9. Example T_{MTRG} image histogram for n = 100 bins

Single white pixels on the image are due to the leather surface texture. In order to remove such tiny effects the binary image is additionally filtered (a pixel equal to 1 is reset to 0 if the mean in its 3x3 neighbourhood is less than 0.3, a pixel equal to 0 is set to 1 if the mean in its neighbourhood is greater than 0.5). The final results, i.e. filtered binary images obtained using the presented algorithm for the equivalent thermogram sequences of leather samples 1-3 are presented in figure 11.

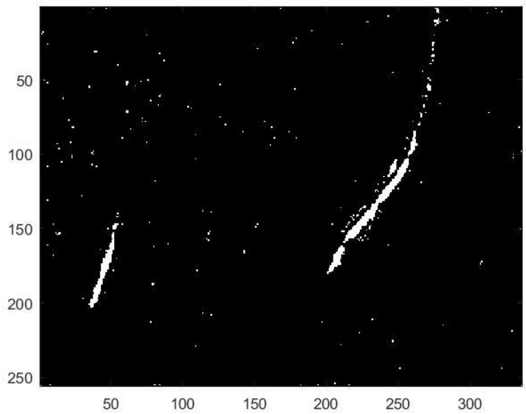

Fig. 10. Binary image obtained for sample 1

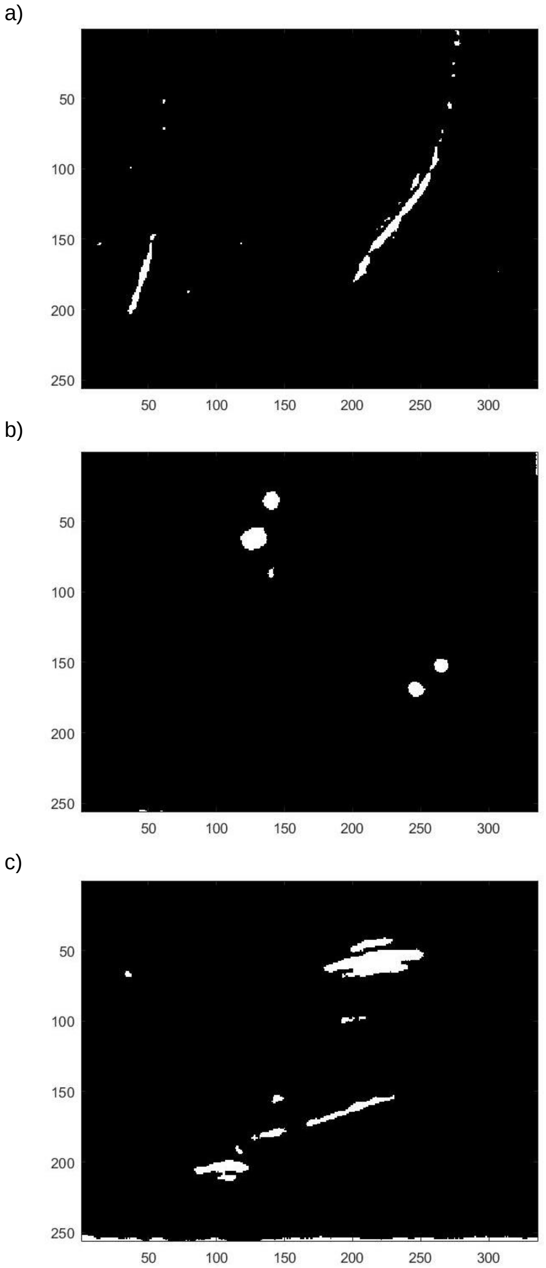

Fig. 11. Image of detected defects obtained for a) sample 1, b) sample 2, c) sample 3

Conclusions

Results obtained from processing of leather surface temperature transients showed that a very important factor is appropriate choice of essential algorithm parameters: blurring filter kernel size d_{xy} and the heat diffusion observation time (processing time horizon) $t(i_p)$.The former parameter is strictly connected with the infrared camera resolution and field of view (FOV). It should be adjusted depending on the leather grain size compared to the whole surface area in the FOV. The heat diffusion observation time $t(i_p)$ should be chosen according to the inspected leather thickness and thermal parameters which depend in turn on an animal, fibrous internal structure and tanning method. Number of bins n of the histogram calculated for maxima image T_{MTRG} affects the determined binarization threshold. Inappropriate choice of n and, in consequence, incorrect binarization, can falsely indicate leather surface grains as defects. Other important factors are: improper settings of the infrared radiator power and travelling speed. Due to inhomogeneity of natural leather, that makes it impossible to determine parameters for a mathematical model of the heat diffusion process [13], the only way is to adjust the processing algorithm parameters empirically.

Defects detected by the presented algorithm coincide with those indicated by experts from the quality department of a renowned manufacturer of upholstered furniture that provided leather samples for testing. The presented, relatively simple, algorithm of thermogram sequence processing in the time domain gives results that are almost as good as those provided by the more complex algorithm based on morphological transformations of selected single thermograms (will be presented in the next publication). The goal of the developed project is to verify the possibility to automate quality evaluation of leather delivered to an upholstered furniture manufacturer. Currently, this process is carried out "manually" by visual inspection. The proposed method, based on forcing the heat flow through the inspected leather, allows for detecting subsurface defects that might be invisible to the naked eye. After implementation of the proposed method the quality control staff would be provided with a single image that could be projected on the inspected leather surface with marked areas of potential defects.

Author: *dr hab. inż. Stanisław Chudzik, Politechnika Częstochowska, Katedra Automatyki, Elektrotechniki i Optoelektroniki, al. Armii Krajowej 17, 42-200 Częstochowa, E-mail: chudzik@el.pcz.czest.pl*

REFERENCES

[1] Farley, M. 40 years of progress in NDT—History as a guide to the future. In AIP Conference Proceedings; AIP Publishing LLC.: Melville, NY, USA, 2014; Volume 1581, p. 5.
[2] Maldague X.: Theory and Practice of Infrared Technology for Nondestructive Testing. John Wiley & Sons, Inc., New York, 2001
[3] Więcek B., Pacholski K., Olbrycht R., Strakowski R., Kałuża M., Borecki, M., Wittchen W., Termografia I Spektrometria w Podczerwieni, WNT, Warszawa, Poland, 2017; ISBN 9788301191870
[4] Minkina, W. Theoretical Basics of Radiant Heat Transfer—Practical Examples of Calculation for the Infrared (IR) Used in Infrared Thermography Measurements. Quant. Infrared Thermogr. J. 2021, 18, 269–282.
[5] Gryś S., Minkina W., Noninvasive Methods of Active Thermographic Investigation: Short Overview of Theoretical Foundations with an Example of Application, Energies 2022, 15, 4865 https://doi.org/10.3390/en15134865
[6] Rogalski A. Infrared Detectors, CRC Press Taylor & Francis Group, 2011, ISBN 978-1-4200-7671-4
[7] Gralewicz G., Owczarek G., Więcek B., Investigations of single and multilayer structures using lock-In thermography – possible applications. JOSE Int. J. Occupat. Saf. Ergon. 11 (2005), 211–215.
[8] Chrysafi A.P., Athanasopoulos N., Siakavellas N.J., Damage detection on composite materials with active thermography and digital image processing, International Journal of Thermal Sciences,116 (2017), 242-253.
[9] Minkina W., Dudzik S.: Infrared Thermography – Errors and Uncertainties. John Wiley & Sons Ltd., Chichester, 2009.
[10] Osornio-Rios, R.A.; Antonio-Daviu, J.A.; De Jesus Romero-Trancoso, R. Recent industrial applications of infrared thermography: A review. IEEE Trans. Ind. Inform. 2018, 15, 615–625.
[11] Gryś, S.; Dudzik, S. Investigation on dual-domain data processing algorithm used in thermal non-destructive evaluation. Quant. Infrared Thermogr. J. 2020, 19, 196–219.
[12] Dudzik S., Two-stage neural algorithm for defect detection and characterization uses an active thermography, Infrared Physics and Technology, 71 (2015), 187-197.
[13] Chudzik S.: Applying infrared measurements in a measuring system for determining thermal parameters of thermal insulation materials, Infrared Physics & Technology 81, 2017, 296–304